Evidence from fluid inclusions for microbial methanogenesis in the early Archaean era

Article *in* Nature · March 2006

DOI: 10.1038/nature04584 · Source: PubMed

5 authors, including:

Yuichiro Ueno
Tokyo Institute of Technology
125 PUBLICATIONS **2,667** CITATIONS

SEE PROFILE

Naohiro Yoshida
Tokyo Institute of Technology
337 PUBLICATIONS **7,447** CITATIONS

SEE PROFILE

Shigenori Maruyama
Tokyo Institute of Technology
520 PUBLICATIONS **17,919** CITATIONS

SEE PROFILE

Yukio Isozaki
The Univeristy of Tokyo
231 PUBLICATIONS **6,967** CITATIONS

SEE PROFILE

LETTERS

Evidence from fluid inclusions for microbial methanogenesis in the early Archaean era

Yuichiro Ueno[1,3,5], Keita Yamada[4,5], Naohiro Yoshida[1,3,4,5], Shigenori Maruyama[1,2] & Yukio Isozaki[6]

Methanogenic microbes may be one of the most primitive organisms[1], although it is uncertain when methanogens first appeared on Earth. During the Archaean era (before 2.5 Gyr ago), methanogens may have been important in regulating climate, because they could have provided sufficient amounts of the greenhouse gas methane to mitigate a severely frozen condition that could have resulted from lower solar luminosity[2] during these times. Nevertheless, no direct geological evidence has hitherto been available in support of the existence of methanogens in the Archaean period, although circumstantial evidence is available in the form of ~2.8-Gyr-old carbon-isotope-depleted kerogen[3]. Here we report crushing extraction and carbon isotope analysis of methane-bearing fluid inclusions in ~3.5-Gyr-old hydrothermal precipitates from Pilbara craton, Australia. Our results indicate that the extracted fluids contain microbial methane with carbon isotopic compositions of less than −56‰ included within original precipitates. This provides the oldest evidence of methanogen (>3.46 Gyr ago), pre-dating previous geochemical evidence by about 700 million years.

The samples came from the Dresser Formation at the North Pole area in Pilbara craton, Western Australia. The Dresser Formation consists of pillowed basaltic greenstones and chert beds. In the North Pole area these rocks have merely undergone low-grade metamorphism below the greenschist facies[4–6]. The lowermost chert unit of the formation is intercalated with several barite beds[4]. This chert–barite unit contains ^{34}S-depleted pyrites, which were presumably produced by sulphate-reducing microbes[7]. The unit also contains one of the oldest putative microfossils[8,9] (see refs 10 and 11 for alternative views).

The minimum depositional age of the Dresser Formation is constrained by the zircon U–Pb age of 3,458 ± 2 Myr for the felsic volcanics that overlie the formation[12]. A model lead age of 3,490 Myr[12] was obtained for galena from the chert–barite unit. This may represent the actual depositional age of the Dresser Formation[13,14].

In the study area, more than 2,000 silica dykes characteristically intruded into the pillowed basaltic greenstones below the chert–barite unit[5,6,9,13,14] (Fig. 1 and Supplementary Fig. S1). These are 0.3–20 m wide and generally more than 100 m in length; the longest is more than 1 km in length. Some silica dykes intruded into the chert beds of the chert–barite unit, but the dykes did not cut through the entire chert–barite unit, nor into the overlying pillow basalt. The top of each dyke exhibits a gradual transition into a certain chert bed, thus forming a T-junction. These relationships indicate that silica dykes might have been formed intermittently during the deposition of the chert–barite beds[9,13,14].

The dykes are composed mainly of fine-grained silica (less than 10 μm) with a smaller amount of sulphides and organic matter (kerogen)[6]. The origin of the kerogen in these dykes is still controversial[15], although their C and N isotope signatures and mode of occurrence imply that they may have been produced by chemoautotrophic organisms[6,16]. Some silica dykes exhibit a symmetrical growth pattern along the dyke axis and occasionally have an agate, in which the silica shows fan-shape structure, grown from the hanging walls towards the centre of the dyke (Fig. 1b, c). These textures and their silica-dominated mineral assemblages indicate the precipitation of silica from a low-temperature (less than 200 °C) hydrothermal fluid[6,13,14].

For the analyses of fluid inclusions we used coarse-grained quartz (more than 1 mm), which shows the same growth directions as those of host silica dykes (see Supplementary Methods for sample selections). Additional samples also came from quartz veins, which are distinguished from the silica dykes by their lack of kerogen and the coarser-grained nature of the quartz. The quartz veins exhibit intrusive patterns similar to adjacent silica dykes; they would therefore have formed contemporaneously with the silica dykes.

All of our quartz samples contain H_2O–CO_2 fluid inclusions (Fig. 1e and Supplementary Fig. S2). The laser Raman spectroscopy of individual fluid inclusions revealed that these fluids consist mainly of H_2O and CO_2 with a minor but detectable amount of CH_4 (see Supplementary Notes).

The fluid inclusions are petrographically classified into types I, II and III on the basis of their distinct mode of occurrence. Type I inclusions occur as clusters along the growth faces of the host quartz, and their distribution patterns often define growth zones of the crystal (Fig. 1d and Supplementary Fig. S2a–d). Individual type I inclusions are 1–15 μm in diameter and are often oriented in the growth direction of host quartz. These textures indicate that type I represents 'primary' inclusion[17], which was entrapped during the growth of host mineral. In contrast, type II inclusions are distributed in the plane of a secondary sealed crack, which often crosscuts more than two quartz crystals (Supplementary Fig. S2e, f). They are typically 1 μm or less in diameter. Type II inclusions are clearly entrapped after the crystallization of the host quartz and correspond to 'secondary' inclusions[17]. Type III inclusions are scattered uniformly in the host quartz without any preferred orientation. They are 5–20 μm in diameter and generally have irregular shapes (Supplementary Fig. S2g, h). Type III inclusions often occur as dense cluster in quartz and show no crack-seal texture. They are therefore probably primary inclusions, although their secondary origin cannot be completely disregarded.

The silica dykes contain type I and II inclusions, whereas the quartz veins contain type II and III. The modal fractions of secondary inclusions (type II) of all the analysed samples vary from less than 0.1 to more than 0.9 (Fig. 2a; see Supplementary Methods).

[1]Research Center for the Evolving Earth and Planet, Tokyo Institute of Technology, [2]Department of Earth and Planetary Science, Tokyo Institute of Technology, Meguro-ku, Tokyo 152-8551, Japan. [3]Department of Environmental Science and Technology and [4]Department of Environmental Chemistry and Engineering, Tokyo Institute of Technology, Midori-ku, Yokohama 226-8503, Japan. [5]SORST project, Japan Science and Technology Corporation (JST), Kawaguchi, Saitama 332-0012, Japan. [6]Department of Earth Science and Astronomy, University of Tokyo, Meguro-ku, Tokyo 153-8902, Japan.

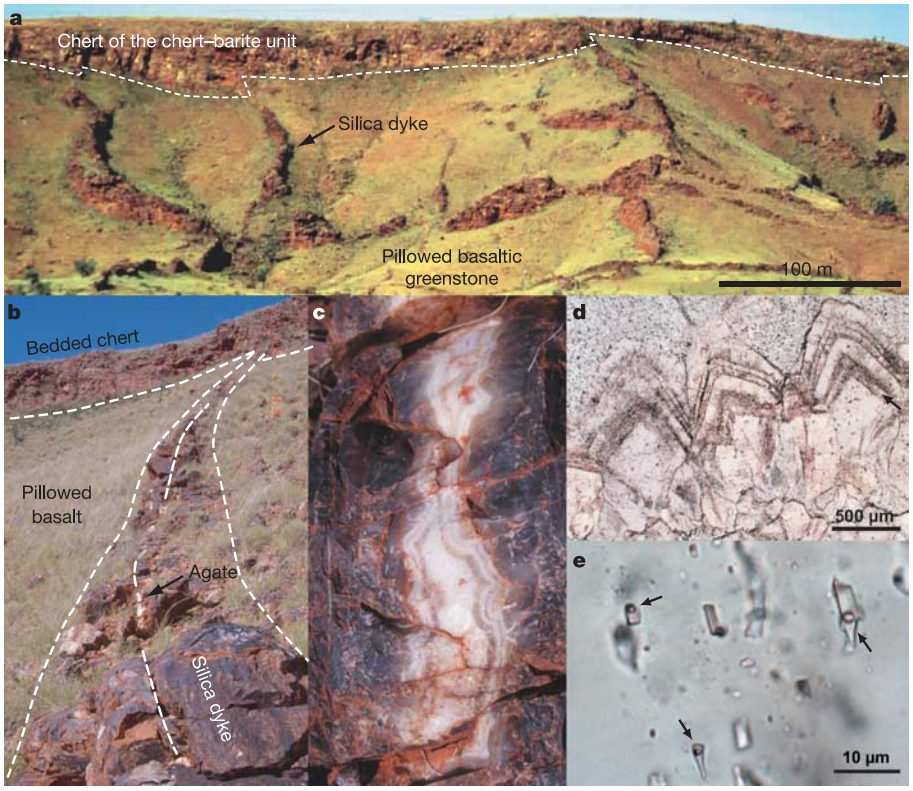

Figure 1 | Photographs of hydrothermal silica dykes and fluid inclusions therein. a, Annotated photograph of the Dresser Formation, showing silica dykes developed in the pillowed basaltic greenstones below the chert–barite unit (above dashed line). **b**, Photograph of an approximately 1-m-wide silica dyke. **c**, Central part of the silica dyke, showing agate and fluid-inclusion-bearing coarse-grained quartz (white portion). The black portion is composed of fine-grained silica with organic matter. The width of the photo is about 15 cm. **d**, Optical photomicrograph of the quartz containing fluid inclusions. Numerous small black dots (arrow) are fluid inclusions distributed along the crystal faces, which define the growth zones of the host quartz. **e**, Enlarged view of the H_2O–CO_2 fluid inclusions (arrows). See also Supplementary Fig. S2 for the types of fluid inclusion.

The fluid inclusion volatiles were extracted from about 1 g of quartz samples by vacuum crushing (Supplementary Methods). Artificially produced CH_4 during crushing was monitored before extraction, and could be ruled out as a source of methane. The $\delta^{13}C$ values of extracted CH_4 and CO_2 are -56 to -36‰ and -7 to 0‰, respectively (Fig. 2 and Supplementary Tables).

The $\delta^{13}C$ values of the extracted CH_4 are correlated with the modal abundance ratios of secondary inclusions (Fig. 2a). ^{13}C-depleted CH_4 is preferentially observed in samples rich in primary inclusions, whereas relatively ^{13}C-enriched CH_4 is observed in those rich in secondary inclusions. The $\delta^{13}C$ values of coexisting CO_2 also exhibit a similar systematic trend and display positive correlation with the $\delta^{13}C_{CH_4}$ values (Fig. 2c). The isotopic variations of the extracted CH_4 and CO_2 can therefore be explained by the mixing of two components: one is primary (that is, entrapped during mineral growth) and the other is secondary (that is, introduced after mineralization). The primary component has ^{13}C-depleted CH_4 and CO_2 ($\delta^{13}C_{CH_4} < -56$‰; $\delta^{13}C_{CO_2} < \sim -4$‰), and the secondary one is more ^{13}C-enriched ($\delta^{13}C_{CH_4} \approx -35$‰; $\delta^{13}C_{CO_2} \approx 0$‰).

The origins of the CH_4 can be deduced by their isotopic compositions. Geological CH_4 has generally been categorized into three groups: microbial (emitted by the metabolic activities of methanogenic microbes), thermogenic (generated by the thermal decomposition of organic matter) and abiotic (produced by non-biological reactions from simple inorganic compounds such as CO_2 and H_2). The $\delta^{13}C_{CH_4}$ value of the secondary component (~ -35‰) is within the proposed range of thermogenic CH_4 (see refs 18 and 19, for example), whereas that of the primary component (less than -56‰) is within the range of mixed gas (that is, a mixture of microbial and thermogenic CH_4 (refs 18, 19)). This empirical comparison is adequate for the first approximation; however, the origin of the methane may be evaluated more explicitly by isotopic fractionation between the methane and potential carbon sources rather than by the $\delta^{13}C_{CH_4}$ values alone.

The CH_4 in the primary component is significantly ^{13}C-depleted relative to the coexisting CO_2 ($\Delta^{13}C_{CO_2 - CH_4} > 52$‰), which is comparable to that exhibited by microbial methanogenesis (Fig. 2b). On the basis of previous culture experiments, it can be stated that CO_2 reduction by methanogenic microbes causes distinctively large fractionations ($\Delta^{13}C_{CO_2 - CH_4} = 30$–$70$‰) (Fig. 2b; see ref. 20 and references therein). Although the fractionation might be smaller under high-temperature hydrothermal conditions, the large fractionation of more than 50‰ has also been observed for hyperthermophilic methanogens grown above 80 °C (ref. 20). Some methanogens can also produce CH_4 by decomposing acetate, which results in fractionations of 7–22‰ between the acetate and CH_4 (ref. 20). If it is assumed that the potential substrate acetate had a $\delta^{13}C$ value similar to that of kerogen in the silica dyke (~ -35‰)[6], the acetate fermentation process can also explain the observed fractionation of the primary component ($\Delta^{13}C_{kerogen-CH_4} > 21$‰). The methane in the primary component is therefore comparable to that produced by methanogenic microbes both by CO_2 reduction and by acetate fermentation.

Alternatively, the thermogenic origin of the primary component should also be considered because the silica dykes contain kerogen[6]. However, the lack of higher hydrocarbons (C_{2+}) in the primary component is inconsistent with its thermogenic origin (Fig. 2b). If the methane is thermogenic in origin, extracted gas should contain C_{2+} along with methane, because thermal decomposition of organic matter yields not only methane but also C_{2+}. With regard to all of the extracted fluids, ethane and propane are below the detection limit ($C_{2+}/(C_1 + C_{2+}) \ll 0.01$), which can be probably attributed to

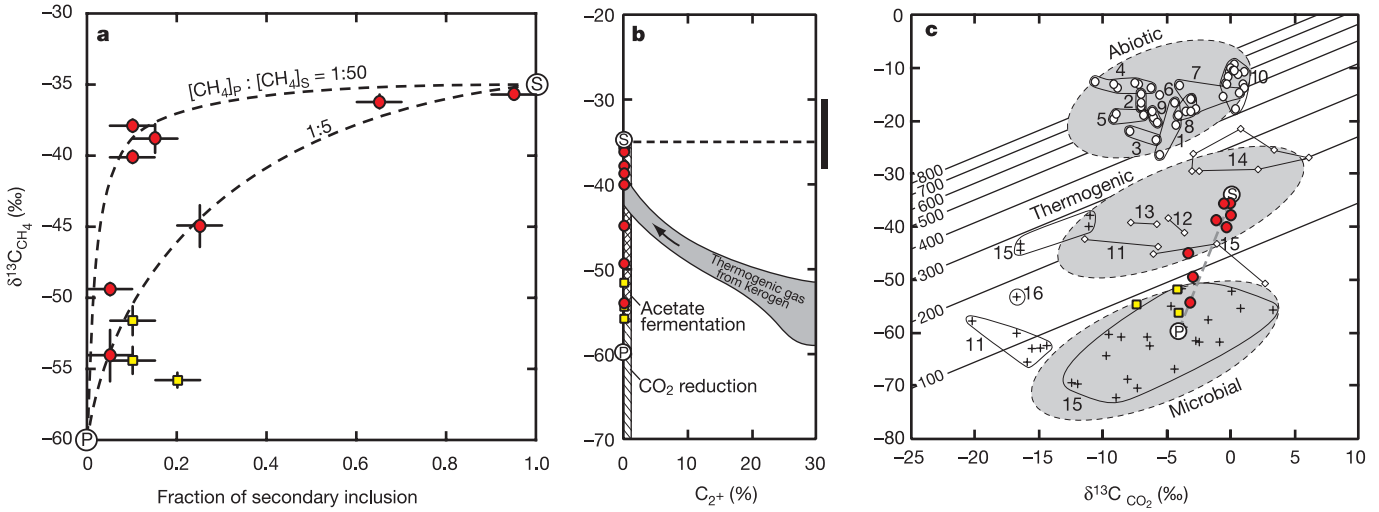

Figure 2 | Carbon isotopic compositions of CH_4 and CO_2 in the fluid inclusions. a, Relationship between carbon isotopic composition of extracted CH_4 and modal fraction of secondary inclusions (type II). Note that type I and III are primary inclusions occurring in silica dykes (circles) and quartz veins (squares), respectively. The two dashed lines represent mixing models between primary and secondary components, assuming that the secondary component contains a CH_4 concentration fivefold or 50-fold that of the primary component. The $\delta^{13}C_{CH_4}$ values of the primary and secondary components are assumed to be −60‰ and −35‰, respectively. See Supplementary Note for error estimates (standard deviation of replicate runs). **b**, $\delta^{13}C$ values of the extracted CH_4 along with the expected $\delta^{13}C_{CH_4}$ − $\%C_{2+}$ ($= 100 \times C_{2+}/(C_1 + C_{2+})$) relationship of hypothetical thermogenic gas derived from kerogen in the silica dykes. The field is calculated from a Rayleigh model[21]. The initial $\delta^{13}C$ value of kerogen is assumed to be −35‰ (dashed line), which is a representative value of kerogen in the silica dykes (black bar[6]). The arrow indicates the directions of the isotopic and compositional changes during the maturation of the host kerogen. The oblique line and cross-hatched fields indicate the calculated ranges of bacterial CH_4 through the CO_2 reduction and acetate fermentation pathways, respectively. The calculations assume that the $\delta^{13}C$ values of substrate CO_2 and acetate are −4 and −35‰, respectively, and fractionations are 30–70‰ for CO_2 reduction and 7–22‰ for acetate fermentation[20]. **c**, Relationship between $\delta^{13}C_{CH_4}$ and $\delta^{13}C_{CO_2}$ values of the extracted fluids in comparison with those of fluids in present-day seafloor hydrothermal systems. Vent gases emitted from unsedimented ridges (circles), sedimented ridges (diamonds) and pore fluid (crosses) are interpreted to be abiotic, thermogenic and microbial, respectively. The number denotes each hydrothermal vent (see Supplementary Notes for data source). Oblique lines represent apparent temperatures in °C, assuming isotopic equilibrium between CO_2 and CH_4 (ref. 27).

their microbial origin. The lack of C_{2+} might result from the decomposition of hydrocarbons into methane. However, if this is so, the $\delta^{13}C_{CH_4}$ value should be close to those of source kerogens[21] and should therefore be much higher than −56‰ (Fig. 2b). Thermogenic origin therefore cannot explain the ^{13}C-depleted isotopic composition of the primary CH_4.

In contrast, the CH_4 in the secondary component has a more ^{13}C-enriched isotopic composition (∼−35‰), which is similar to those of kerogens in silica dykes[6] (Fig. 2b). This isotopic similarity along with the lack of C_{2+} indicates that the CH_4 might be matured thermogenic gas derived from the adjacent kerogen, although its microbial origin cannot be completely disregarded.

Last, we must consider the possibility that non-biological processes such as Fischer–Tropsch-type (FTT) reactions[22–24] might have produced the methane. Previous experimental work has indicated that Fe–Ni-alloy-catalysed FTT reactions in hydrothermal systems can produce methane with isotopic compositions similar to those observed in this study[22], but these results have not been duplicated[23]. Moreover, Fe–Ni alloys and other catalysts for FTT reactions would not have existed in the surrounding rocks at temperatures prevailing during silica precipitation[5,6]. The abiotic origin of the extracted CH_4 is therefore controversial.

Indeed, abiotic methane is emitted from various present-day seafloor hydrothermal vents[25,26] and has a highly ^{13}C-enriched isotopic composition ($\delta^{13}C_{CH_4} = -26$ to −9‰), which is distinctively higher than those of our extracted fluids (Fig. 2c). Instead, the isotopic composition of the primary component is rather similar to those of the pore fluids in the upper part of the oceanic crust inhabited by methanogens, whereas the secondary component is similar to vent gases emitted from sedimented ridges, which are considered to be thermogenic gases (Fig. 2c). These comparisons also support the microbial origin of the primary CH_4 and the thermogenic origin of the secondary CH_4.

Thus, the fluid inclusions in the more than 3.46-Gyr-old hydrothermal silica dykes contain microbial CH_4 produced by methanogens and entrapped during the formation of the dyke. After precipitation of the host quartz, thermogenic CH_4 from thermal decomposition of the surrounding organic matter might also have been introduced into the dykes. The results of this study provide the oldest evidence of microbial methanogenesis (more than 3.46 Gyr ago), which pre-dates previous geochemical evidence[3] by about 700 Myr.

Furthermore, our results demonstrate the antiquity of the Archeal domain in the universal tree of life, which is formulated by a comparison of ribosomal RNA sequences of extant organisms[1] (Supplementary Fig. S3). Methanogenesis occurs only in the Euryarchaeota, a branch of the Archaea. We therefore suggest that the domains Archaea and Bacteria would have branched from each other at least 3.46 Gyr ago. The antiquity of methanogen supports the hypothesis that microbial CH_4 would have had an important role in regulating the climate on the Archaean Earth[2].

Received 22 August 2005; accepted 10 January 2006.

1. Woese, C. R. Bacterial evolution. *Microbiol. Rev.* **51,** 221–271 (1987).
2. Kasting, J. F. & Catling, D. Evolution of a habitable planet. *Annu. Rev. Astron. Astrophys.* **41,** 429–463 (2003).
3. Hayes, J. M. in *Early Life on Earth* (ed. Bengtson, S.) 220–236 (Columbia Univ. Press, New York, 1994).
4. Buick, R. & Dunlop, J. S. R. Evaporitic sediments of Early Archean age from the Warrawoona Group, North Pole, Western Australia. *Sedimentology* **37,** 247–277 (1990).
5. Kitajima, K., Maruyama, S., Utsunomiya, S. & Liou, J. G. Seafloor hydrothermal alteration at Archean mid-ocean ridge. *J. Metamorph. Geol.* **19,** 583–600 (2001).
6. Ueno, Y., Yoshioka, H., Maruyama, S. & Isozaki, Y. Carbon isotopes and petrography of kerogens in ∼3.5-Ga hydrothermal silica dikes in the North Pole area, Western Australia. *Geochim. Cosmochim. Acta* **68,** 573–589 (2004).
7. Shen, Y., Buick, R. & Canfield, D. E. Isotopic evidence for microbial sulphate reduction in the early Archaean era. *Nature* **410,** 77–81 (2001).

8. Awramik, S. M., Schopf, J. W. & Walter, M. R. Filamentous fossil bacteria from the Archean of Western Australia. *Precambr. Res.* **20,** 357–374 (1983).
9. Ueno, Y., Isozaki, Y., Yurimoto, H. & Maruyama, S. Carbon isotopic signatures of individual Archean microfossils (?) from Western Australia. *Int. Geol. Rev.* **43,** 196–212 (2001).
10. Buick, R. Microfossil recognition in Archean rocks: an appraisal of spheroids and filaments from a 3500 M.Y. old chert-barite unit at North Pole, Western Australia. *Palaios* **5,** 441–491 (1990).
11. Garcia Ruiz, J. M. *et al.* Self-assembled silica-carbonate structures and detection of ancient microfossils. *Science* **302,** 1194–1197 (2003).
12. Thorpe, R. I., Hickman, A. H., Davis, D. W., Mortensen, J. K. & Trendall, A. F. in *The Archaean: Terrains, Processes and Metallogeny* (eds Glover, J. E. & Ho, S. E.) 395–406 (Univ. Western Australia Publ. 9, Perth, 1992).
13. Nijman, W., de Bruijne, K. H. & Valkering, M. E. Growth fault control of Early Archaean cherts, barite mounds and chert-barite veins, North Pole Dome, Eastern Pilbara, Western Australia. *Precambr. Res.* **95,** 247–274 (1999).
14. Van Kranendonk, M. J. & Pirajno, F. Geochemistry of metabasalts and hydrothermal alteration zones associated with c. 3.45 Ga chert and barite deposits: implications for the geological setting of the Warrawoona Group, Pilbara Craton, Australia. *Geochem. Explor. Envir. Anal.* **4,** 253–278 (2004).
15. Brasier, M. D. *et al.* Questioning the evidence for Earth's oldest fossils. *Nature* **416,** 76–81 (2002).
16. Pinti, D. L., Hashizume, K. & Matsuda, J. Nitrogen and argon signatures in 3.8 to 2.8 Ga metasediments: clues on the chemical state of the Archean ocean and the deep biosphere. *Geochim. Cosmochim. Acta* **65,** 2301–2315 (2001).
17. Roedder, E. *Fluid Inclusions* (Reviews in Mineralogy vol. 12, Mineralogical Society of America, Washington DC, 1984).
18. Schoell, M. Genetic characterization of natural gas. *Am. Assoc. Petrol. Geol. Bull.* **67,** 2225–2238 (1983).
19. Whiticar, M. J. Carbon and hydrogen isotope systematics of bacterial formation and oxidation of methane. *Chem. Geol.* **161,** 291–314 (1999).
20. Valentine, D. L., Chidthaisong, A., Rice, A., Reeburgh, W. S. & Tyler, S. C. Carbon and hydrogen isotope fractionation by moderately thermophilic methanogens. *Geochim. Cosmochim. Acta* **68,** 1571–1590 (2004).
21. Clayton, C. Carbon isotope fractionation during natural gas generation from kerogen. *Mar. Petrol. Geol.* **8,** 232–240 (1991).
22. Horita, J. & Berndt, M. E. Abiogenic methane formation and isotopic fractionation under hydrothermal conditions. *Science* **285,** 1055–1057 (1999).
23. McCollom, T. M. & Seewald, J. S. A reassessment of the potential for reduction of dissolved CO_2 to hydrocarbons during serpentinization of olivine. *Geochim. Cosmochim. Acta* **65,** 3769–3778 (2001).
24. Sherwood Lollar, B., Westgate, T. D., Ward, J. A., Slater, G. F. & Lacrampe-Couloume, G. Abiogenic formation of alkanes in the Earth's crust as a minor source for global hydrocarbon reservoirs. *Nature* **416,** 522–524 (2002).
25. Welhan, J. A. Origin of methane in hydrothermal systems. *Chem. Geol.* **71,** 183–198 (1988).
26. Charlou, J. L., Donval, J. P., Fouquet, Y., Jean-Baptiste, P. & Holm, N. G. Geochemistry of high H_2 and CH_4 vent fluids issuing from ultramafic rocks at the Rainbow hydrothermal field (36°14′N, MAR). *Chem. Geol.* **191,** 345–359 (2002).
27. Richet, P., Bottinga, Y. & Javoy, M. A review of hydrogen, carbon, nitrogen, oxygen, sulphur, and chlorine stable isotope fractionation among gaseous molecules. *Annu. Rev. Earth Planet. Sci.* **5,** 65–110 (1977).

Supplementary Information is linked to the online version of the paper at www.nature.com/nature.

Acknowledgements We thank M. Terabayashi, Y. Kato, K. Okamoto, T. Ota, T. Kabashima, K. Kitajima and K. Shimizu for assistance in field work, A. Thorne, K. J. McNamara and A. H. Hickman for field collaboration, H. Nara, Y. Matsui and M. Nishizawa for assisting in the construction of the vacuum line, and R. Buick and J. F. Kasting for comments on early versions of this manuscript. This research was supported by the 21st Century COE Program 'How to build habitable planets,' Tokyo Institute of Technology, sponsored by the Ministry of Education, Culture, Sports, Technology and Science, Japan. Y.U. thanks the Research Fellowships of the Japan Society for the Promotion of Science for Young Scientists.

Author Information Reprints and permissions information is available at npg.nature.com/reprintsandpermissions. The authors declare no competing financial interests. Correspondence and requests for materials should be addressed to Y.U. (yueno@depe.titech.ac.jp).